Ilka Weikusat[1],
Atsushi Miyamoto[2], Sérgio H. Faria[4], Gill M. Pennock[3], Nobuhiko Azuma[5],
Takeo Hondoh[2], Martyn R. Drury[3], Sepp Kipfstuhl[1]

(9-P-40) PCI 2010, Sapporo, September 5 to September 10

# Dislocation Activity in Antarctic ice (EDML core)

[1]Alfred-Wegener-Institut für Polar- und Meeresforschung (Germany), ilka.weikusat@awi.de, [2]Institute of Low Temperature Science (Japan), [3]Utrecht University (The Netherlands), [4]University of Göttingen (Germany), [5]Nagaoka University of Technology (Japan)

## Introduction

As subgrain boundaries (subGB) are comprised of dislocations, orientation of subGB depends on the orientation of the locally active slip systems. Dislocation types can be determined by combined studies on orientation and misorientation (MO) geometries of subGB. SubGB are characterized by (1) orientation within the crystal, (2) MO angle and (3) MO rotation axis.

## Methods

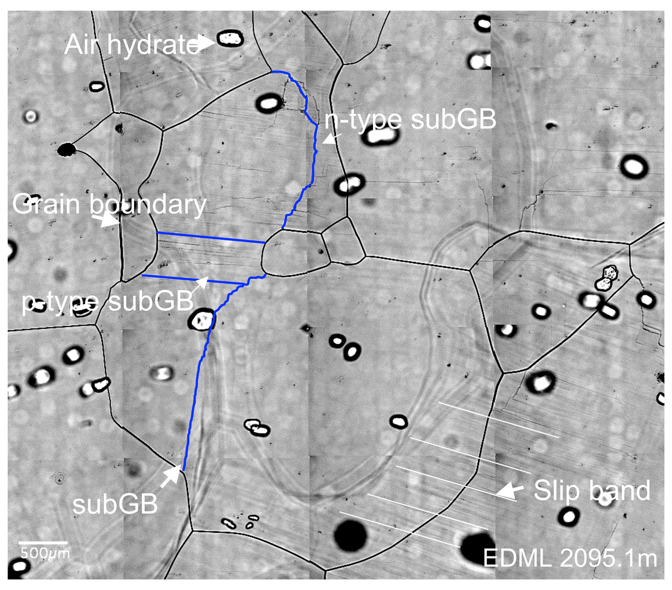


Microstructure Mapping (μSM) using light microscopy[1]

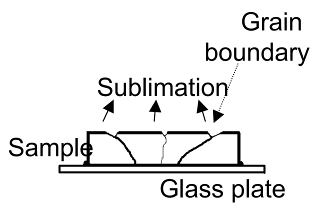


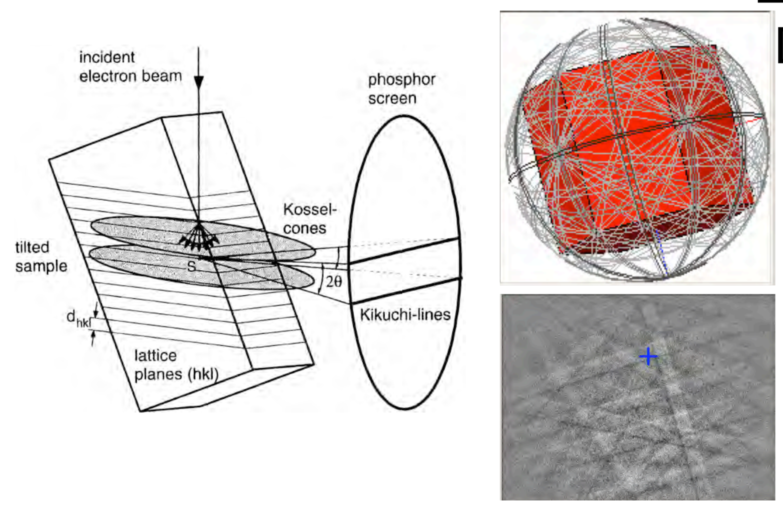


Electron BackScatter Diffraction (EBSD)[2]

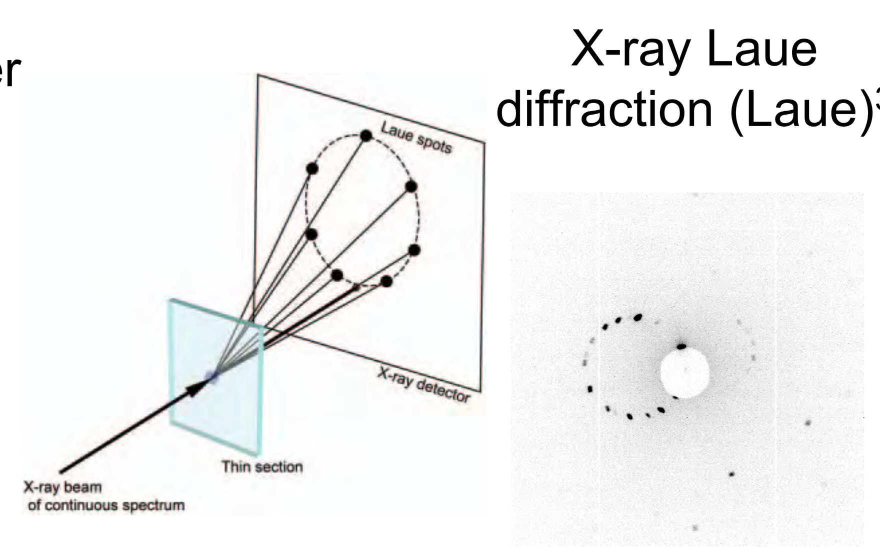


X-ray Laue diffraction (Laue)[3]

## Laue Results and Interpretation[4]

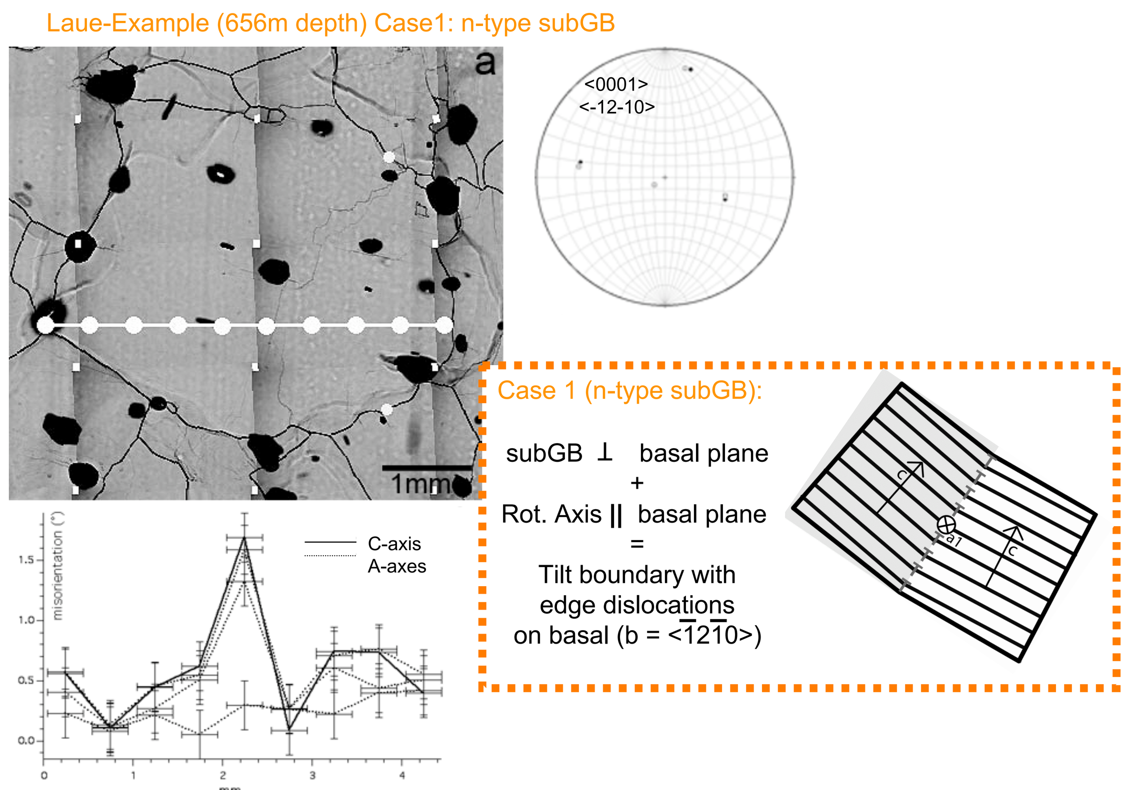


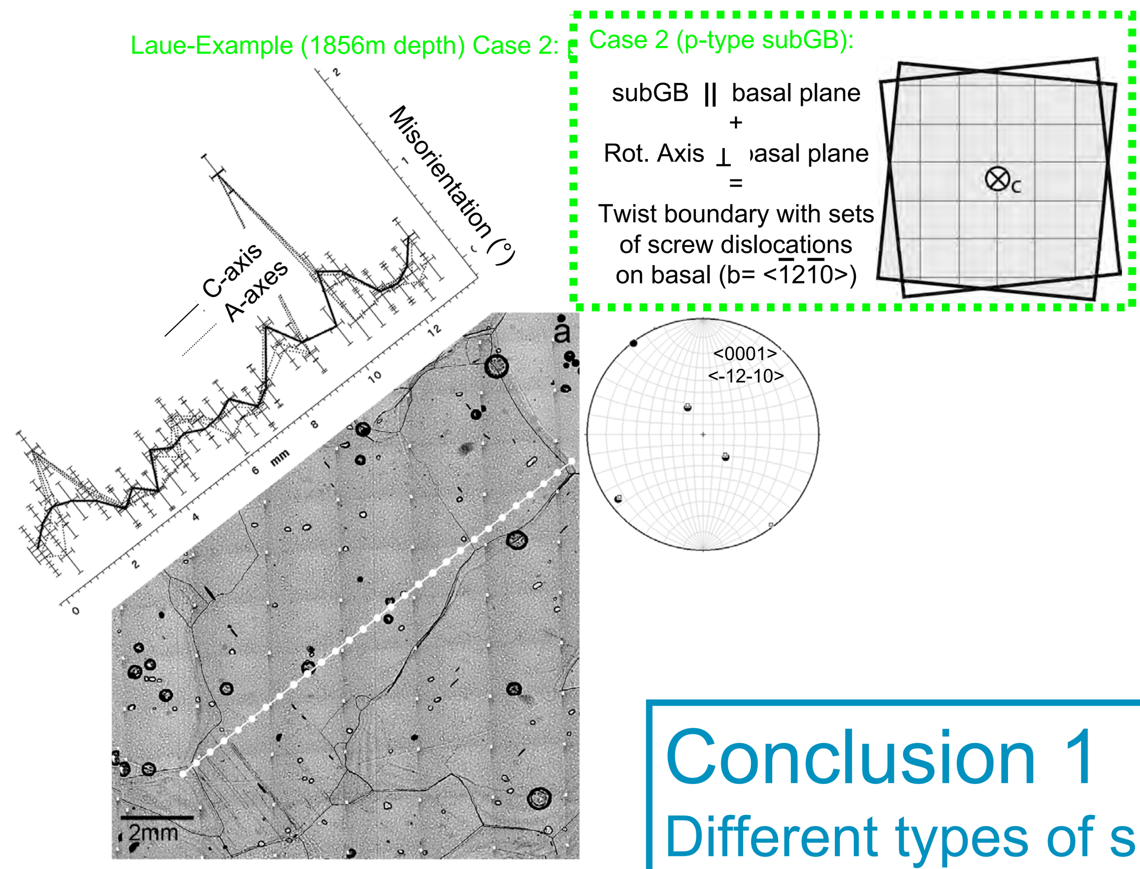


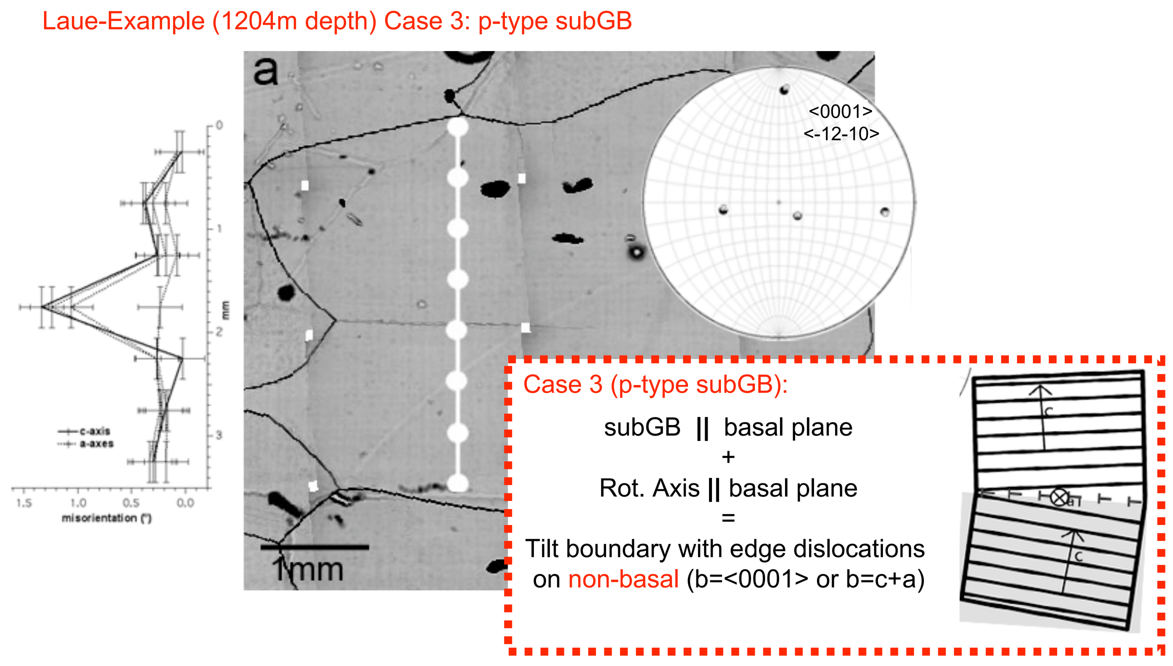


### Conclusion 1

Different types of subGB (Cases 1 to 3) are found based on their geometric characteristics. The relevant dislocations to form these subGB types can be deduced. Surprisingly, dislocations gliding on non-basal planes are very frequent (Table 1).

Table 1: Laue data simplified statistics, EDML 18 samples, depths 113 to 2701m. Absolute number frequencies of all subGBs with detectable misorientations ($n_{>0.5°}$ = 165) displaying combined information on misorientation rotation axes (columns) and subGB arrangements (lines).

| Rotation Axis: / Arrangement: | c-axis as rotation axis | rotation axis in basal plane | arbitrary rotation axes |
|---|---|---|---|
| basal plane normal (n and z-type) | 0 | 65[a] | 14 |
| basal plane parallel (p-type) | 11[b] | 45[c] | 14 |
| no particular arrangement to basal plane | 1 | 7 | 8 |

Table 2: EBSD data simplified statistics, EDML 4 samples, 14 EBSD maps, depth 656m. Absolute number frequencies of all subGBs with detectable misorientations ($n_{>0.5°}$ = 196) displaying combined information on misorientation rotation axes (columns) and subGB arrangements (lines).

| Rotation Axis: / Arrangement: | c-axis as rotation axis | rotation axis in basal plane | arbitrary rotation axes |
|---|---|---|---|
| basal plane normal (n and z-type) | 2 | 56[a] | 15 |
| basal plane parallel (p-type) | 7[b] | 54[c] | 15 |
| no particular arrangement to basal plane | 7 | 28 | 14 |

## EBSD Results and Interpretation

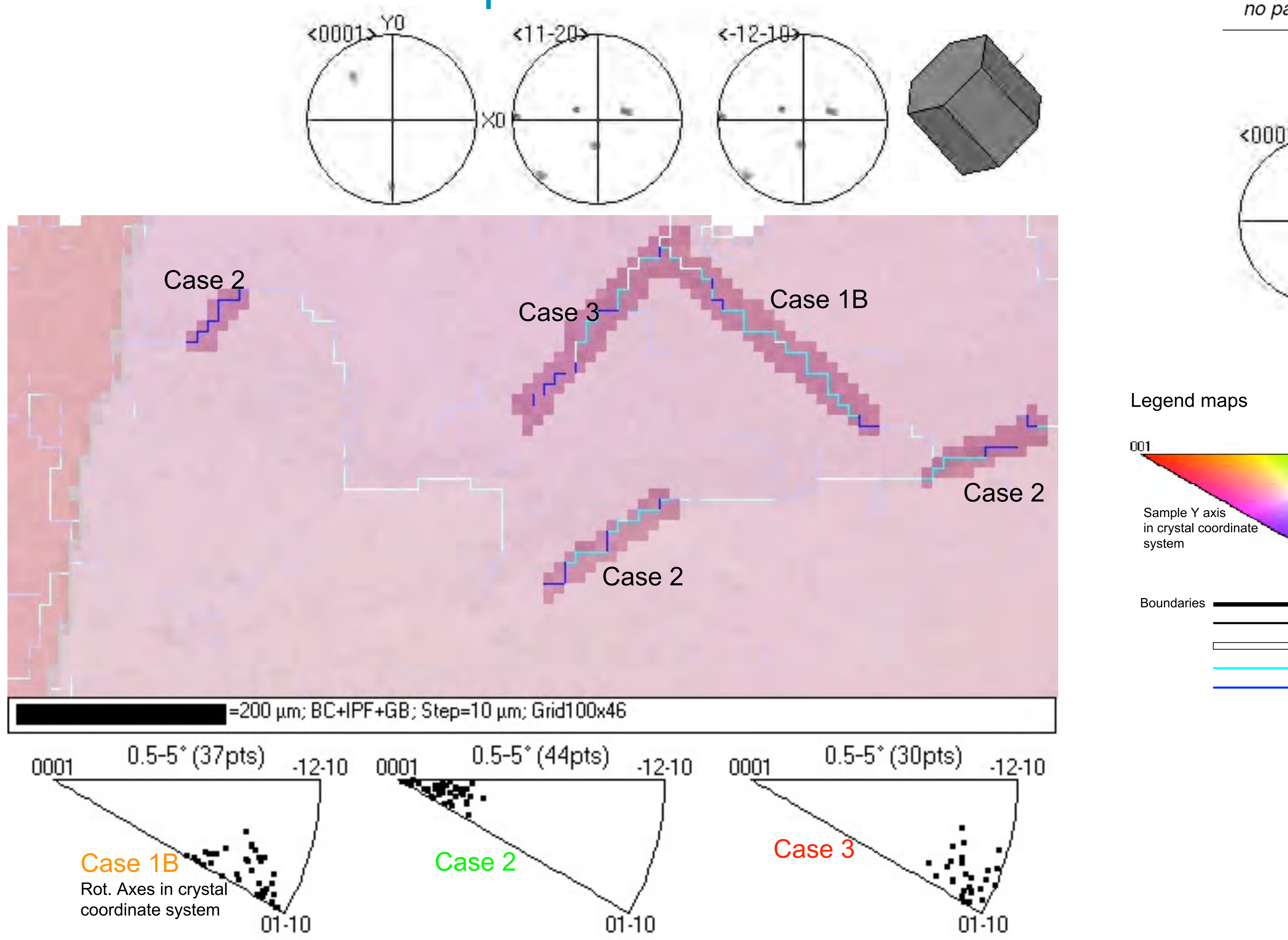


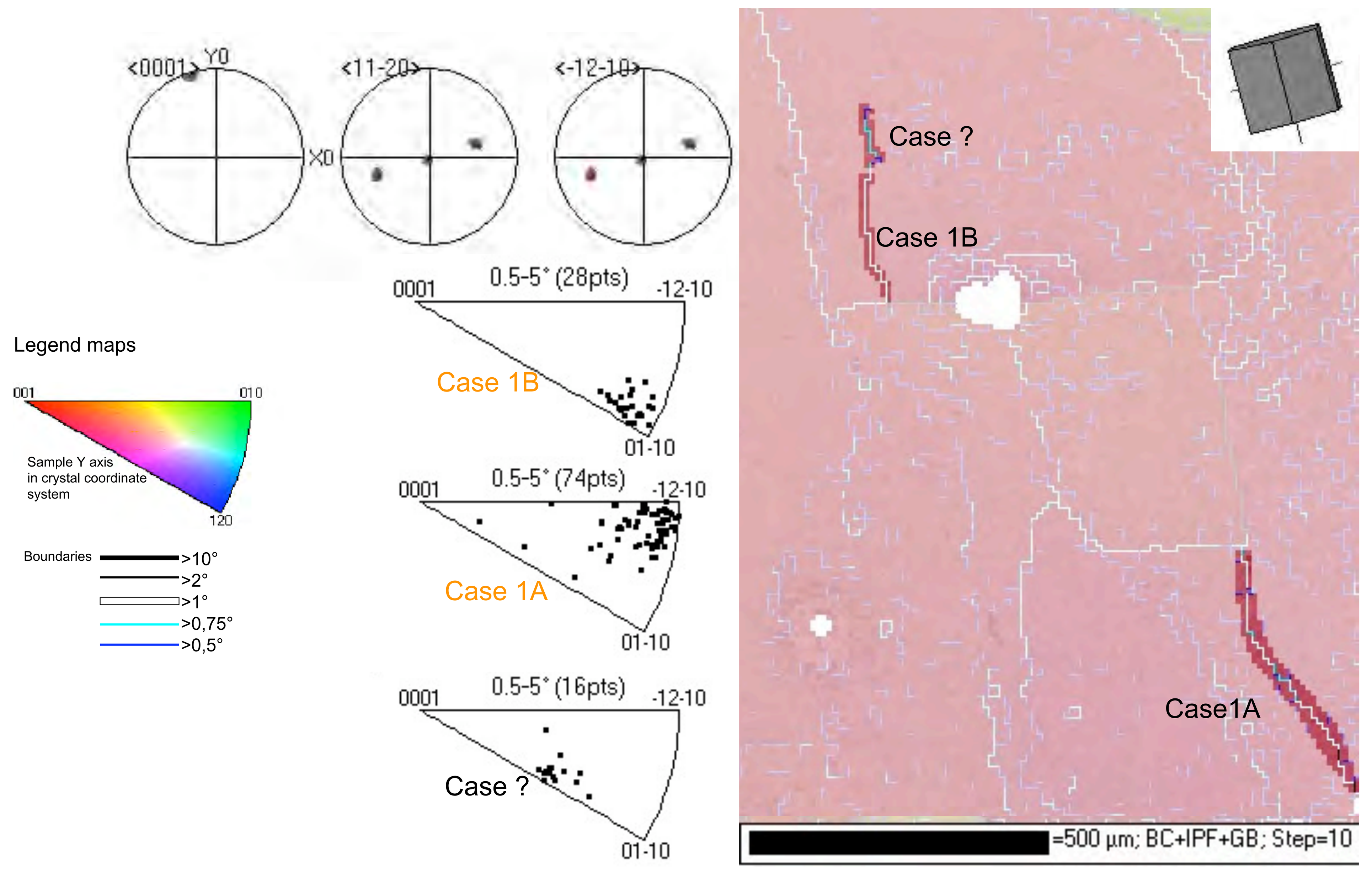


Table 3: EBSD data statistics, EDML 4 samples, 14 EBSD maps, depth 656m. Absolute number frequencies of all subGBs with detectable misorientations ($n_{>0.5°}$ = 196 ) displaying combined information on misorientation rotation axes (columns) and subGB arrangements (lines).

| Rotation Axis: / Arrangement: | $<0001>$ c-axis | $<\bar{1}2\bar{1}0>$ a-axis | $<01\bar{1}0>$ prism-normal | $<xxx0>$ in basal plane | $<\bar{1}011>$ pyr.-normal | arbitrary rotation axes |
|---|---|---|---|---|---|---|
| basal plane normal (n and z-type) | 2 | 10[d] | 19[e] | 27[a] | 1[f] | 14 |
| basal plane parallel (p-type) | 7[b] | 8[c] | 11[c] | 35[c] | 2 | 13 |
| no particular arrangement to basal plane | 7 | 9 | 5 | 14 | 0 | 14 |

[a] Case 1: tilt boundary with dislocations in the basal plane
[b] Case 2: twist boundary with dislocations in the basal plane
[c] Case 3: tilt boundary with dislocations in a non-basal plane
[d] Case 1A
[e] Case 1B
[e] Case ?

### Conclusion 2

The high frequency of non-basal dislocations is confirmed by EBSD (Table 2). Further different types of tilt boundaries with basal dislocations are observed (Case 1A & B). Surprisingly, mixed boundaries with arbitrary rotation axes can show specific rotation axes close to the pyramidal plane normal (Case ?, Table 3).

References

[1]Kipfstuhl, S.; Hamann, I.; Lambrecht, A.; Freitag, J.; Faria, S.; Grigoriev, D. & Azuma, N. Microstructure mapping: a new method for imaging deformation induced microstructural features of ice on the grain scale J. Glaciol., 2006, 52, 398-406
[2]Randle, V. & Engler, O. Introduction to texture analysis: Macrotexture, Microtexture and Orientation Mapping. Taylor & Francis, 2000, 388
[3]Miyamoto, A.; Shoji, H.; Hori, A.; Hondoh, T.; Clausen, H. & Watanabe, O. Ice fabric evolution process understood from anisotropic distribution of a-axis orientation on the GRIP (Greenland) ice core. Ann. Glaciol., 2005, 42, 47-52
[4]Weikusat, I.; Miyamoto, A.; Faria, S. H.; Kipfstuhl, S.; Azuma, N. & Hondoh, T. Subgrain boundaries in Antarctic ice quantified by X-ray Laue diffraction, in press, J. Glaciol., 2010